Flying Qualities Assessment Using Nonlinear Frequency Response Analysis

Duc H. Nguyen[1], Mark H. Lowenberg[2], Simon A. Neild[3], and Thomas S. Richardson[4]
Department of Aerospace Engineering, University of Bristol, Bristol, BS8 1TR

Current methods of assessing flying qualities are based on linear system theory, which cannot capture the nonlinear phenomena commonly found at high angles of attack. Although bifurcation analysis has been proven to be a powerful tool for numerically analyzing nonlinear flight dynamics, in its standard (unforced) form, the method is unsuitable for flying qualities assessment as no information on the transient response is provided. To address this shortcoming, we propose the use of an extension of bifurcation analysis that treats the aircraft as a harmonically forced system. This facilitates the evaluation of the frequency-domain dynamics where the response is unsteady by definition. It is shown that the method can identify regions with strong nonlinearities that lead to degraded flying qualities. Time simulations of the closed-loop step responses in these undesirable regions show that despite the predictions of desirable behaviors using linear analysis, the closed-loop aircraft can still be attracted to an isola, experience control reversal, or have higher overshoot than anticipated.

Nomenclature

A	=	forcing amplitude (deg)
q	=	pitch rate (deg/s)
t	=	time (s)
x	=	general state vector
α	=	angle of attack (deg)
η	=	elevator deflection (deg)
ω	=	forcing frequency (Hz or rad/s)
Subscripts		
d	=	demanded
$trim$	=	value at trimmed (steady) flight

I. Introduction

Linear-based controllers remain in widespread use in many nonlinear closed-loop applications including aircraft flight control systems. One of the ways in which nonlinearity is accounted for when using linear design methods is gain scheduling, in which the gain values are calculated at a number of different operating points and then combined into a single controller with the intention of achieving stability and consistent performance across the operating envelope. Although this controller can satisfy the performance criteria, the method and the criteria themselves remain a locally linear-based solution. It has been shown that in some nonlinear situations, the controller fails to achieve the desired response. An example can be found in [1], which uses an aircraft gain-scheduled maneuver-demand controller designed to have the same closed-loop pole positions across the entire operating envelope. The local performance is satisfactory (near the point on which the controller is designed), suggesting that the controller performs well. However, when the aircraft is forced to move across different operating points, there are cases where the controller not only fails

[1] PhD student, AIAA Student Member.
[2] Professor of Flight Dynamics, AIAA Senior Member.
[3] Professor of Nonlinear Structural Dynamics.
[4] Senior Lecturer in Flight Mechanics, AIAA Senior Member.

to achieve the desired transient response but is also unable to take the aircraft to the commanded position. Another example appears in [2], which also shows a few instances of the controller failing to prevent the aircraft from entering a spin outside the normal operating envelope. In both cases, the cause can be attributed to the increased aerodynamic nonlinearity in the aircraft model (or "plant" using control terminology) as it moves further away from the design point of the controller considered. Meanwhile, many aircraft design and handling quality criteria are still linear-based [3, 4]. Therefore, they are subject to the limitations of linear system theories. More research needs to be done to construct a framework to assess aircraft flying qualities that can capture the nonlinear effects.

In an effort to bridge the gap between the linear and nonlinear domains, there has been increasing interest in utilizing nonlinear analysis on aerospace applications in the past few decades. The use of bifurcation analysis with numerical continuation is well established [2, 5, 6] and has proven to be a powerful tool that can capture the nonlinear nature of flight dynamics. Bifurcation analysis generates a map of the steady-state solutions as a parameter, such as elevator deflection, is varied. Highly nonlinear behaviors like spin and autorotation can be captured and represented as stable and unstable steady state solutions. This approach has its limits, most notably the inability to capture the transient behavior since only final steady-state solutions are shown. In practical terms, this means the method is very useful in identifying regions where the dynamics is unacceptable and should be avoided, and helping to identify magnitudes of disturbances for which an attracting solution remains stable, but not in assessing an aircraft performance (such as damping ratio variations) when in transient motion between different stable solutions. To capture the time-dependent effects during transient responses while still doing the analysis on the full nonlinear model, there have been some investigations into generating periodic solutions by coupling the aircraft with a harmonic forcing terms [7-9]. This is a promising approach, but more research is needed due to the complexity involved in studying a nonlinear periodically forced system, which is so far only common in weakly nonlinear theoretical systems [10-12]. For detailed descriptions of the methods, readers are referred to [13, 14] for basic bifurcation analysis, [15] for bifurcation analysis in periodically forced systems, and [16, 17] for typical examples of its flight dynamics applications.

This paper aims to further exploit the advantages of bifurcation analysis with numerical continuation to assess the aircraft flying quality without relying on linear system theory. By generating periodic solutions of the closed-loop aircraft in response to a harmonic input, information on the flying characteristics in the frequency domain can be obtained (from this point referred to as the nonlinear frequency response). Periodic solutions are non-stationary by definition, which provides a new perspective on the aircraft dynamic that might be overlooked using conventional unforced bifurcation analysis. In addition, as this nonlinear frequency response is obtained using the full nonlinear equations of motion, it can be used to assess the influence of nonlinearities across the aircraft's wide operating envelope, and hence allow the flying qualities at different operating points to be compared.

II. Aircraft model

The method presented in this paper is demonstrated on the Hypothetical High Angle of Incidence Research Model (HHIRM) created for the Defence Research Agency in the UK (now QinetiQ) [18]. The model is made up of six aerodynamic force and moment coefficients, which are nonlinear functions of the angle of attack and sideslip angle. These are represented by spline functions rather than tabular data in order for the system to be smooth (differentiable), making the model highly suitable to be used as a testbed for bifurcation-based methods. The longitudinal 2nd-order version, which contains two states α (angle of attack in degrees) and q (pitch rate in degrees/s) to capture the short-period mode, is used in this paper. Its dynamics is representative of a typical fighter aircraft. Using the reduced-order model restricts the case study to longitudinal dynamics, where only the fast mode is important, and allows for easier interpretation of the results. However, the approach developed in this paper is not limited to such low-order systems.

The HHIRM behavior is highly nonlinear. Figure 1 shows the open-loop bifurcation diagrams with the elevator deflection η on the x-axis as the continuation parameter. These diagrams are the equilibria sets for the two states α and q as functions of η. It can be seen that due to the fold bifurcations, there are three solutions in the region -20^o $\leq \eta \leq$ -10^o. From a practical perspective, this means that:

- For -20^o $\leq \eta \leq$ -10^o, the aircraft has two equilibrium states: one at a lower and one at a higher (deep stall) angle of attack. Whichever solution the aircraft converges to will depend on the initial conditions.

- It is not possible to manually trim the aircraft at angles-of-attack between 34^o and 46^o because the solutions in that range are unstable.

Three different controllers for the 2nd-order HHIRM are proposed in [1, 19], all of which aim to stabilize the aircraft and ensure consistent handling qualities across the whole α range. The controllers are designed using various linear and nonlinear design methods while also accounting for a first-order actuator described by equation (1).

$$\frac{\eta}{\eta_d} = \frac{30}{s+30} \tag{1}$$

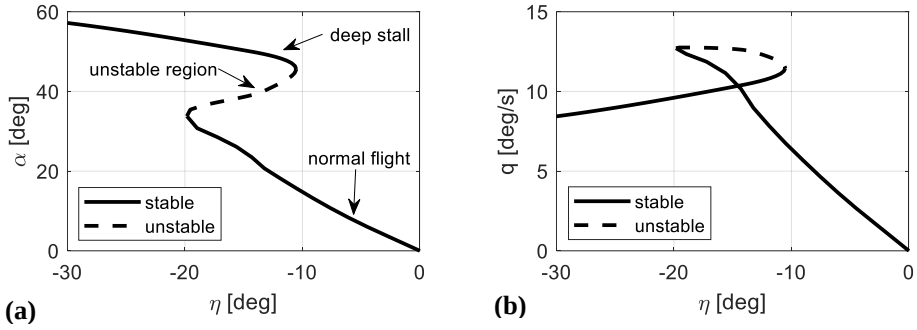

Fig 1 Open-loop bifurcation diagram – elevator continuation.

In the sections to follow, the performances of these three controllers are analyzed using the proposed method.

III. Nonlinear frequency response analysis

All analysis presented in the sections to follow is closed-loop and the reference signal is the demanded angle-of-attack α_d. To generate a harmonic input signal for nonlinear frequency response analysis, we augment our third-order system of three states $[\alpha, q, \eta]$ with two additional states:

$$\dot{x}_4 = x_4 + \omega x_5 - x_4(x_4^2 + x_5^2) \tag{2}$$
$$\dot{x}_5 = x_5 - \omega x_4 - x_5(x_4^2 + x_5^2) \tag{3}$$

where ω is the forcing frequency in rad/s. It can be shown that $x_4 = \sin(\omega t)$ and $x_5 = \cos(\omega t)$. The reference signal will now take the form:

$$\alpha_d = \alpha_{trim} + A\sin(\omega t) = \alpha_{trim} + Ax_4 \tag{4}$$

where A (deg) is the forcing amplitude.

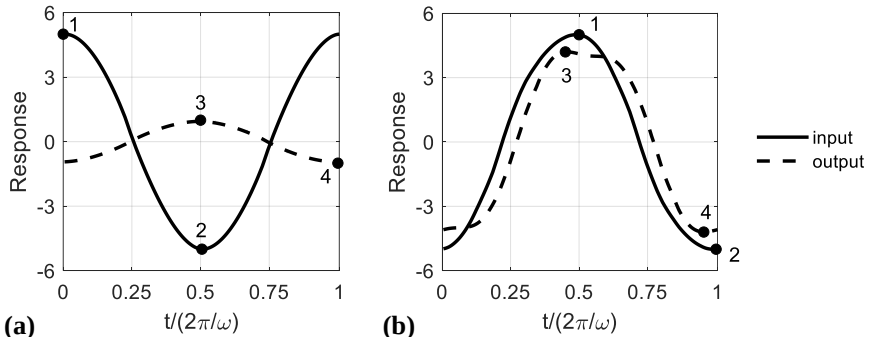

Fig 2 Examples of periodic solutions generated using AUTO.

Periodic solutions are generated numerically in the MATLAB environment using the Dynamical Systems Toolbox [20], which is a MATLAB implementation of the bifurcation analysis software AUTO [21]. It is known that in a highly nonlinear system, these solutions can contain multiple harmonics such as in Figure 2b. In those cases, we define the gain and phase relationships between the input and the output as:

$$gain\ in\ dB = 20\ log_{10}\left(\frac{Y_3 - Y_4}{Y_1 - Y_2}\right) \tag{5}$$

$$phase\ in\ degree = (X_1 - X_3) \times 360 \tag{7}$$

where X_i and Y_i refer to the x and y-coordinates of point i in Figure 2. It will be shown later that this way of defining the phase is very useful in detecting regions with significant nonlinearities, which often result in responses with multiple harmonics such as the case seen in Figure 2b.

IV. Analysis of the feedforward controller

A. Controller architecture and known issues

In the first example, we chose a controller in which only proportional gains are used to show how this architecture is not sufficient to overcome the influence of a secondary attractor. Figure 3a shows the schematic block diagram of the feedforward controller described in [1]. In essence, this is an output feedback controller that incorporates a feedforward path to scale the reference signal and create a maneuver demand system. The feedforward signals are shown in Figure 3b and were calculated by inverting the open-loop bifurcation diagrams in Figure 1 so that, given the demanded angle-of-attack α_d, the elevator deflection and pitch rate at trim η_{trim} and q_{trim} are found. The feedback gains are scheduled against the pilot's input α_d as shown in Figure 3c and were calculated using eigenstructure assignment, which places the short-period poles at one fixed location throughout the entire operating envelope (α between 0º and 60º). Although it is possible to schedule the gains with the measured α rather than α_d, doing so would introduce other problems in matching desired responses as it effectively modifies the system Jacobian matrix [22].

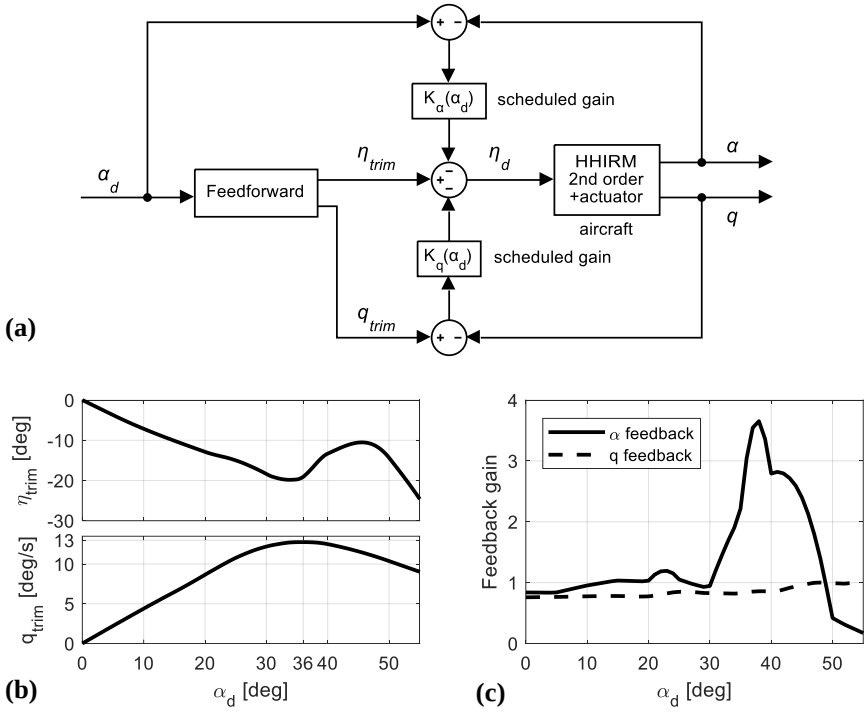

Fig 3 (a) feedforward controller block diagram, (b) feedforward signals, (c) and scheduled feedback gains.

It has been shown in [1] that local performances in the form of small-amplitude step responses are desirable and similar across the entire operating envelope. However, some large step inputs cause the aircraft to respond in an undesirable manner. This can be explained by examining the closed-loop unforced α bifurcation diagram (Figure 4). The purpose of scaling the input signal is so that there is a 1:1 mapping between the input α_d and the resulting angle of attack α, which is reflected by the main stable branch Figure 4: a straight line showing a linear dependency of these two variables. However, there exist an isola (a second branch that is not connected to the main one) with stable solutions near α = 50º. The stable solutions in the isola create the second and undesirable attractor that will influence the aircraft dynamics. For instance, a reference signal of α_d = 50º will converge to one of the two angles of attack: the demanded α = 50º or the undesirable α = 32º that originated from the isola. The initial conditions will determine which solution the aircraft converges to.

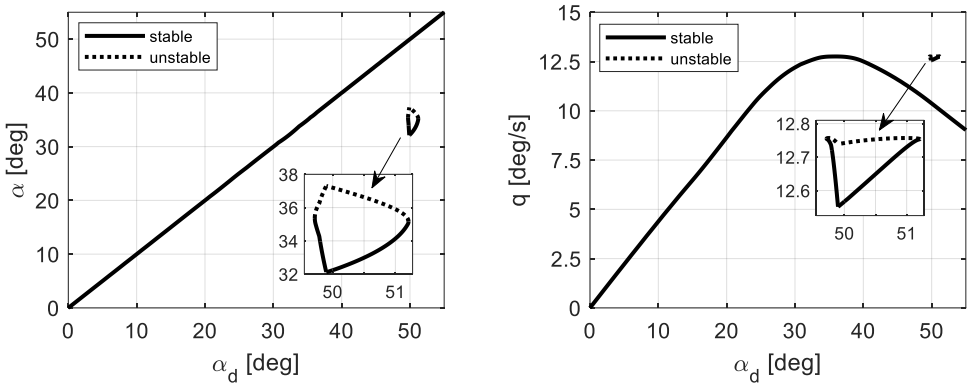

Fig 4 Bifurcation diagrams of α_d against α and q.

The influence of the isola can be studied by examining the three step responses in Figure 5a along with their phase plots in Figure 5b. The first case (30º to 34º) is desirable. In the second case (α_d steps from 30º to 50º), the trajectory lands on the isola at α = 32º instead of the commanded position. The final case (30º to 54º) reaches the commanded position, but the response is erratic and does not resemble the usual short period mode. Examining the phase plot shows that in the third case, the trajectory is attracted to the stable isola before carrying on to its final destination at 54 deg, indicating that the isola is having a deleterious effect on the transient dynamics. Although demanding a step response of this magnitude is unrealistic for most aircraft, the effect of the isola on the aircraft's trajectory is still noticeable even when a smoother input is used. In this case, the step input was chosen to present the worst-case scenario, as often done in control studies. The principal purpose of this example is to exemplify the problem and the proposed analysis approach.

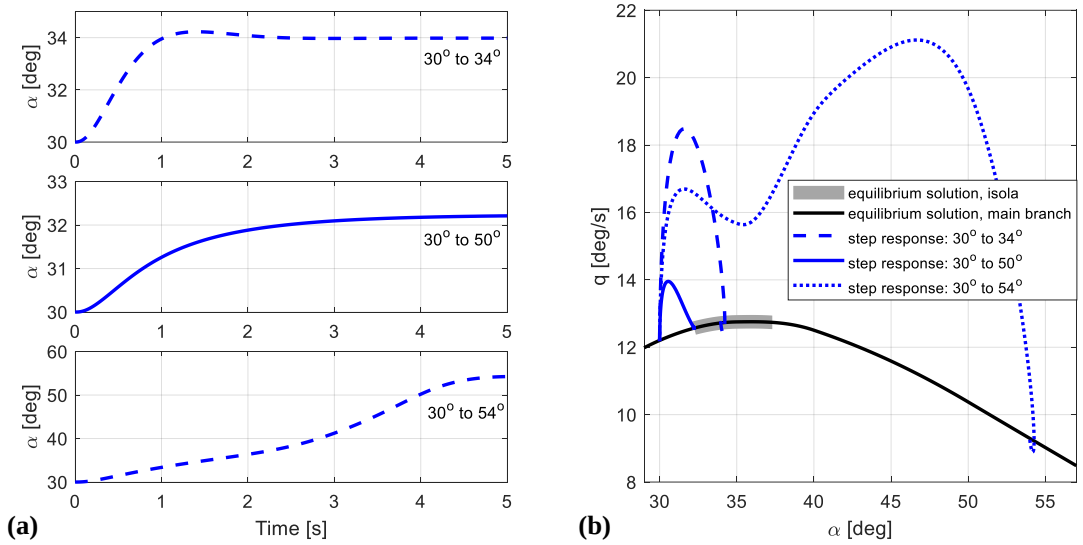

Fig 5 (a) step responses and (b) phase plots.

We have seen that the presence of the isola can influence the aircraft response if its trajectory approaches the affected region. The next section will show how nonlinear frequency response analysis can be used to quantify this influence on the aircraft flying qualities and help to detect regions of highly nonlinear behavior caused by the existence of the isola.

B. Flying qualities assessment

We will now examine the trimmed aircraft at α_{trim} = 30º. Firstly, the nonlinear closed-loop frequency responses with three forcing amplitudes A are considered: 1º, 4º and 24º, corresponding to α_d sweeps between [29º, 31º], [26º, 34º] and [6º, 54º] (as a reminder, $\alpha_d = \alpha_{trim} + A\sin(\omega t)$ for the forced response). The first two cases were chosen

as examples of the aircraft undergoing maneuvers fairly local to its equilibrium condition, and the third case corresponds to type of challenging large-amplitude input that will be influenced by the isola as discussed above.

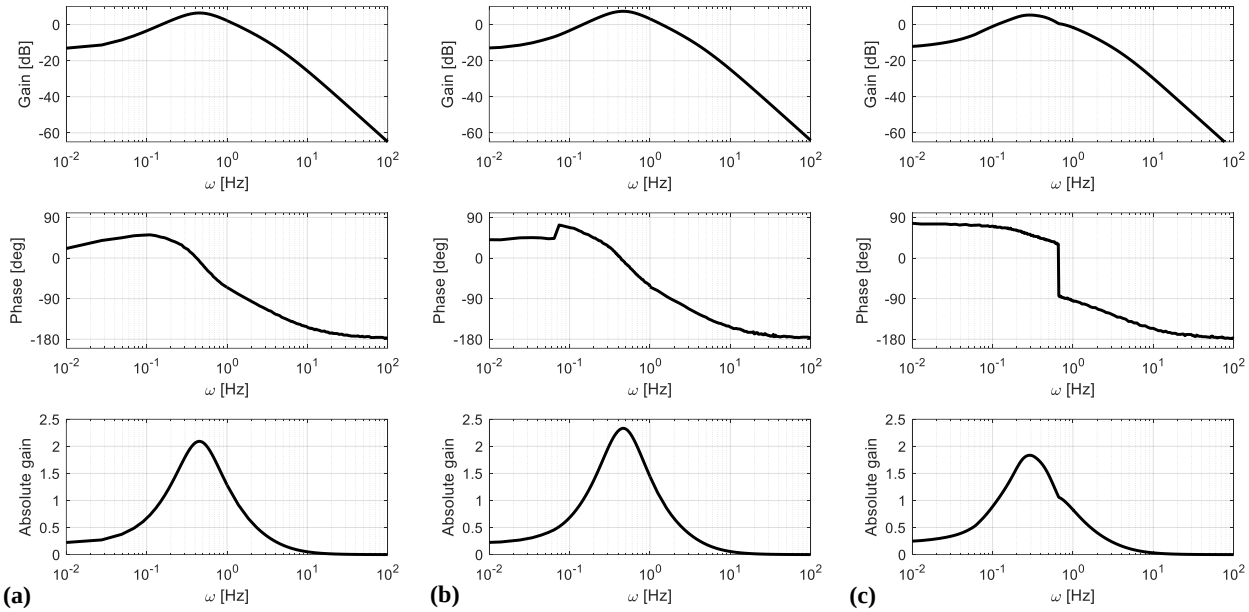

Fig 6 Nonlinear α_d-to-q frequency responses for (a) A = 1º, (b) A = 4º, and (c) A = 24º.

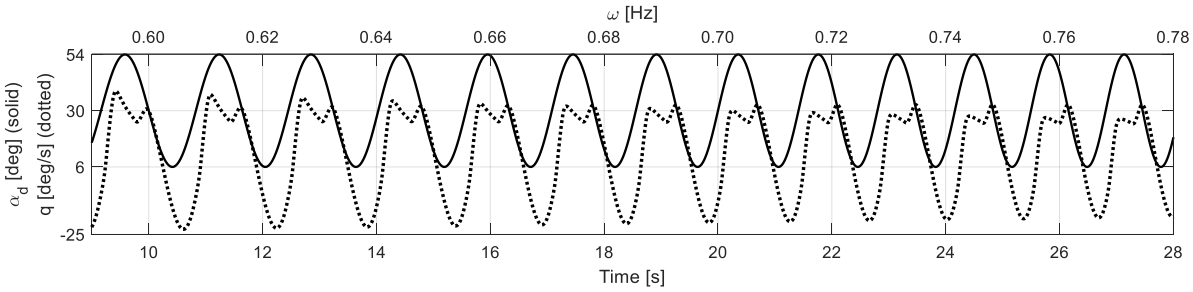

Fig 7 Simulated forced response at A = 24º with a chirp signal.

The nonlinear q-to-α_d frequency responses are shown in Figure 6. For A = 1º, the frequency response resembles that of a linear transfer function, suggesting that the aircraft behaves like a linear system in this region. In the second case with A = 4º, a phase jump is seen at 0.06 Hz. Increasing A to 24º will lead to a more abrupt phase jump at a higher frequency of 0.66 Hz in addition to causing a distortion in the gain response, which can be seen more clearly in the absolute gain diagram (instead of the dB gain diagram). To verify the phase jump in the third case, the aircraft is simulated with a chirp signal so that the forcing frequency ω increases linearly while the forcing amplitude A is kept constant at 24º. Figure 7 shows that the pitch rate response is highly nonlinear and has two separate peaks in each cycle. To explain the shape of the pitch rate response observed, it is useful to refer back to the second panel of Figure 3b, which shows the equilibrium relationship between α_d and q_{trim}. If the forcing frequency is low enough such as in the case of Figure 7, the aircraft's states will trace along their equilibria. It can be seen in Figure 3b that beyond α_d = 36º, increasing α_d will lead to a reduction in q, and this is reflected in the time history of Figure 7 when α_d exceeds 36º, leading to the formation of the first peak. Similarly, the second peak is formed when α_d changes direction and drops below 36º again. The asymmetry of the pitch rate response leads to its distorted shape in the gain diagram. The phase jump seen in Figure 6c is therefore caused by our current definition for phase, which is the normalized time between the forcing peak and the highest response peak (equation 7). We can see from Figure 7 that as the forcing frequency increases, the highest pitch rate peak switches from the left one to the right one, which is captured as a phase jump on the frequency response. In practical terms, this method of generating the nonlinear frequency response can provide an indication as to when the aircraft operates in a nonlinear region, which in this case is caused by the nonlinear relationship between α_d and q.

The α_d-to-α frequency responses are shown in Figure 8 for three different values of A. All three instances look very similar and show 0 dB gain and 0° phase at low frequencies, suggesting the controller achieves the tracking task as long as ω is not too high. Their time histories under a 0.1 Hz forcing frequency are shown in Figure 9. Although the α tracking is acceptable in the first two cases, the third case shows an unusual shape that resembles the step input in Figure 5a (panel 3). Moreover, its pitch rate response is very complicated and clearly shows that the aircraft's trajectory is being affected by the isola that lies along the α_{demand} travelling range. The influence of the isola is also reflected in the magnified view of the gain diagram in the α_d-to-α frequency response – shown as an inset in Figure 8. Here, the frequency response at A = 24° has a reduced bandwidth (defined as the frequency at which the gain drops below -3 dB) comparing to the other two cases, which are less affected by isola as seen from their time histories.

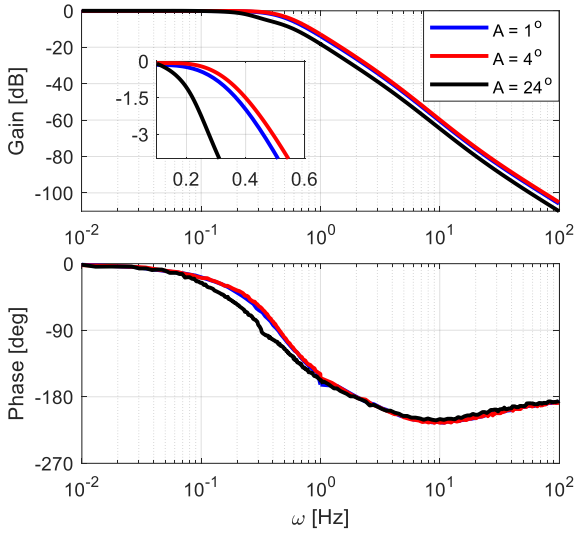

Fig 8 α-to-α_{demand} frequency responses.

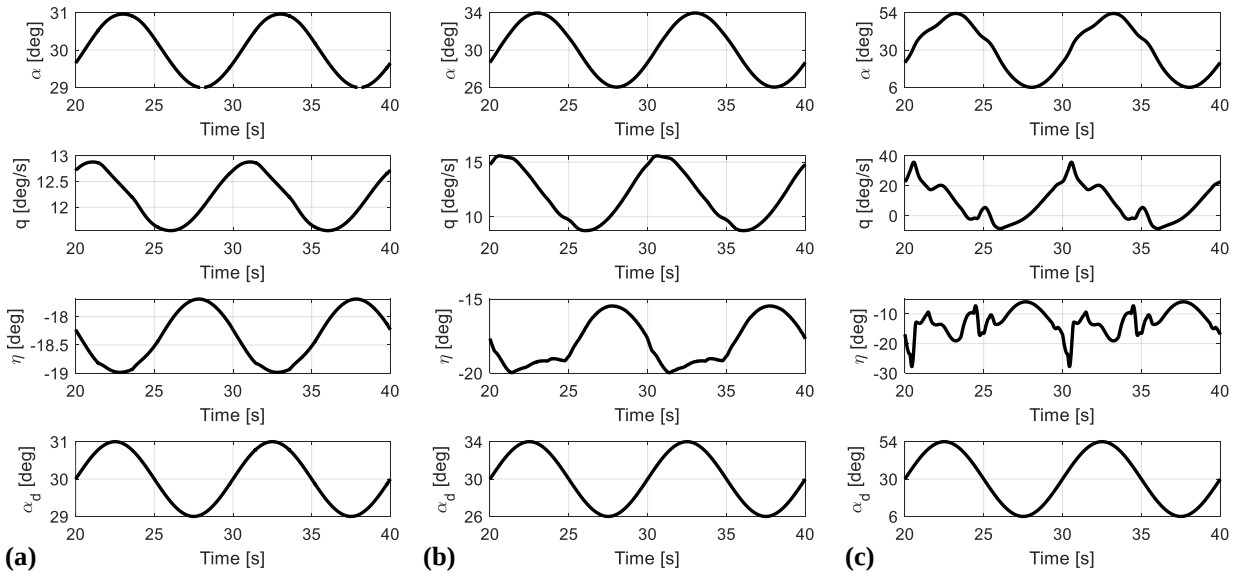

Fig 9 Simulated response to a 0.1 Hz harmonic input with amplitudes (a) 1°, (b) 4°, (c) 24°.

It has been established that the step response from 30° to 54° is heavily affected by the isola and this may also be the cause for the reduced bandwidth in its corresponding frequency response at A = 24°. To verify this, we compare the bandwidth of the closed-loop frequency responses for a range of A and α_{trim}. The result is shown in Figure 10a, which has a triangular shape due to the constraint $0° \leq \alpha_{demand} \leq 60°$ (the controller has not been designed to operate in the negative α_{demand} region, which limits the area of the envelope in Figure 10a). The colors represent the

bandwidth of the closed-loop frequency response. There is a noticeable bandwidth reduction in the region $30^o \leq \alpha_{trim} \leq 50^o$ due to the presence of the isola, which is shown as a red area in Figure 10a. Although the unforced bifurcation diagram in Figure 4 indicates that the isola only exists over a small region of $49.7^o \leq \alpha_d \leq 51.2^o$, the triangular envelope in Figure 10a suggests that the isola affects the aircraft's response over a much larger area.

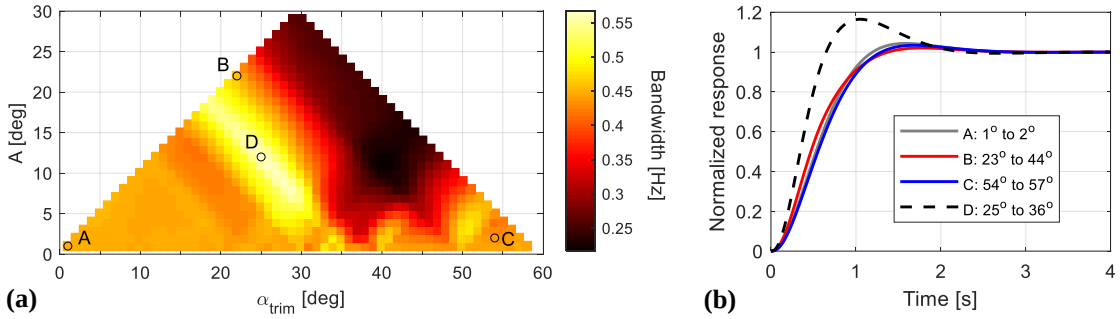

Fig 10 Feed forward controller: (a) closed-loop bandwidth variation and (b) step responses.

Although the diagram Figure 10a was generated using the harmonic input, it can be used to determine if the time-domain behavior is desirable. Specifically, we can predict whether different step responses from α_{trim} to $(\alpha_{trim} + A)$ are similar based on their corresponding colors in the triangular envelope. For example, it can be inferred that the step responses at the points A, B, and C resemble each other because they have similar bandwidths. Figure 10b confirms this observation, despite the facts that the points are very far apart on the envelope and that point B is a very demanding input.

Apart from the red and brown regions, the envelope in Figure 10a also shows an additional yellow area that suggests a different dynamics comparing to those found in the other two regions. The step respond at point D is shown as the dotted line in Figure 10b, which has noticeably higher overshoot and does not resemble the other three cases.

We have seen that aerodynamic nonlinearities can have significant effects on the aircraft responses in both the time and the frequency domains. Using nonlinear frequency response analysis, we have presented a method to quantify these effects. The information gained from the triangular envelope can be used to verify whether consistence handling qualities are achieved across different operating regions. It is important to point out that the purpose of the triangular envelope is not to compare the closed-loop bandwidth but to indicate that bandwidth might be used as a metric to quantify the differences in the frequency response at different operating points. For a more complex system with multiple peaks, the engineer can come up with a different metric, such as resonance peak or estimated damping of each mode, depending on the application considered.

V. Analysis of the controller with an integral path

A. Controller architecture and known issues

Instead of using pre-calculated feedforward data to drive the error signal to zero, the second controller in [1] utilizes an integrator in the forward path, which adds the benefit of guaranteeing the uniqueness of the solution and therefore remove the isola. We present the analysis in this section to show that even though the isola no longer exist due to the integral action, the underlying nonlinearities can still affect the aircraft dynamics in a way that linear-based design fails to recognize. The block diagram and gain scheduling data are shown in Figure 11. Like the first controller, the gains are still scheduled against the pilot's input α_d and the design objective is still placing the short-period poles at the same location across the operating envelope.

It has been reported in [1] that the isola mentioned in the previous section ceases to exists using the current controller. Two step responses that can be considered close to ideal are shown as the solid lines in Figures 12a and 12b. However, the first author of [1] also encountered a few instances of undesirable behavior in which the elevator moves in the opposite direction at the beginning [23]. Two such examples are shown as the dotted lines in Figures 12a and 12b. The case presented in Figure 12b with extremely small step amplitude is chosen to emphasize the fact that the problem is still encountered even when the aircraft operates very locally. This undesirable control reversal behaviors occur near $\alpha_{trim} = 30^o$ – the same region that had been heavily affected by the isola in the previous example – but only when the step input is sufficiently small. Larger step inputs near $\alpha_{trim} = 30^o$ that previously landed on the isola or showed an erratic behavior now resemble the ideal response.

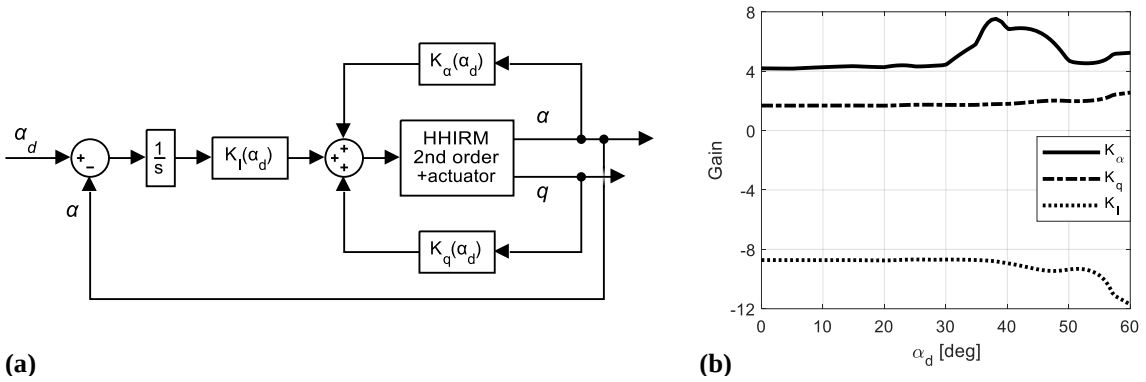

(a) **(b)**

Fig 11 Block diagram (a) and gain scheduling (b) – Output feedback controller with integral action.

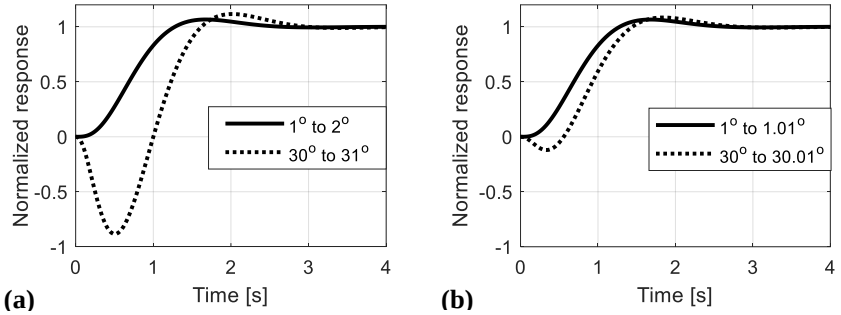

(a) **(b)**

Fig 12 Step responses of the second controller.

B. Flying quality assessment

The closed-loop frequency response at α_{trim} = 30° and A = 0.01° is now examined in Figure 13. As mentioned, the small forcing amplitude is chosen to ensure the nonlinear response is local and comparable to the linearized results. However, Figure 13 shows that there is a noticeable discrepancy between them. In particular, as the forcing frequency increases, the nonlinear response has higher gain but lower phase than its linearized counterpart – a highly nonlinear phenomenon that resembles neither an additional pole nor a zero in the transfer function. Based on its unusual frequency response, it can be said that the behavior in this region cannot be captured by a linear transfer function, which can be linked back to the control reversal in the time-domain response seen in Figures 12b.

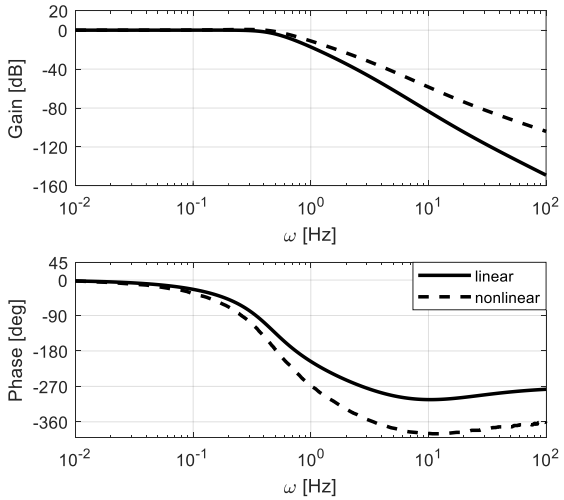

Fig 13 Closed-loop frequency response at α_{trim} = 30° and A = 0.01°.

The triangular envelope is now generated, once again using bandwidth as the metric, to determine the region in which inputs result in nonlinear responses. Figure 14 suggests that control reversal of varying degree may be encountered within the area labelled A. In addition, there is an apparent second nonlinear region labelled B that is separate from A. We investigate this by generating the frequency and step responses from 48° to 48.01° (Figure 15), which is the most affected operating point within B. In the frequency response, the nonlinear analysis has a notably higher resonance that the linear prediction, suggesting that the nonlinear step response will have a much higher overshoot, a fact that is confirmed in Figures 15b. The higher resonance leads to an increase in bandwidth, which is reflected by the area B in Figure 14. Based on the shape of the nonlinear frequency response, it is inferred that the linearized response needs an additional zero in its transfer function in order to capture the dynamics adequately.

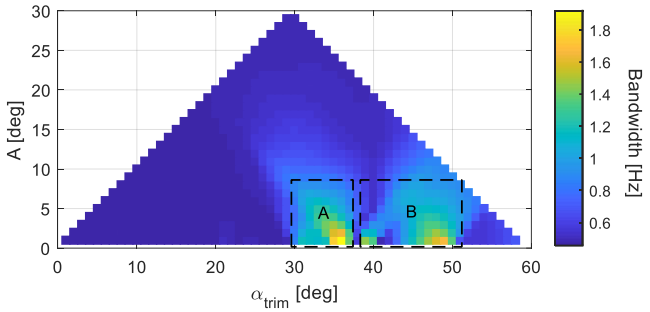

Fig 14 Closed-loop bandwidth variation – feedback with integral action controller.

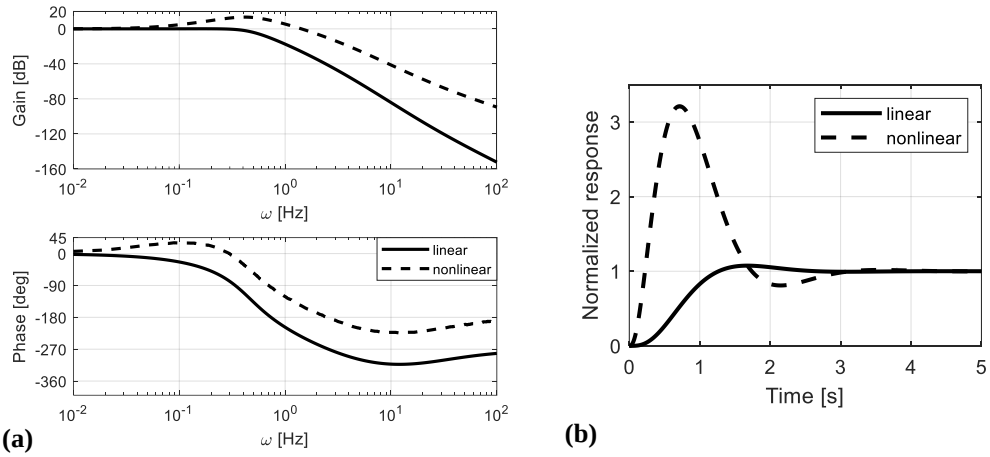

Fig 15 (a) frequency response at α_{trim} = 48° and A = 0.01° and (b) step response from 48° to 48.01°.

VI. Analysis of the dynamic gain scheduled controller

For the final study, the performance of the dynamic gain scheduled controller in [19] is examined. This controller has superior performance comparing to the previous two cases and is presented in this section to ensure that the proposed method does not give false-positive results (i.e. predicting a problem when there is none). The controller has the same architecture as the output feedback controller with integral action presented above (Figure 11) but the feedback gains are scheduled against the outputs themselves (i.e. $K_\alpha(\alpha)$ and $K_q(q)$). It has been shown in [19] that dynamic gain scheduling gives improved transient performance and can address the problems encountered in static gain scheduling with fast-varying state variables, especially when the aircraft maneuvers rapidly across different operating points.

In this example, $K_\alpha(\alpha)$ has been calculated for the whole operating envelope from 0° to 60° whereas $K_q(q)$ is only calculated up to α = 36°. Despite this limitation, we generated the triangular envelope for $0° \leq \alpha_d \leq 60°$ in Figure 16a. A boundary is defined for the region in which dynamic gain scheduling is available for both K_α and K_q. Outside this boundary, only K_α is dynamically scheduled while K_q is fixed at its maximum value calculated from the dynamic

scheduling. It is clear that the performance is superior comparing to static gain scheduling as no undesirable regions is found inside the fully-scheduled boundary. Additionally, the reduced performance outside this boundary is not as severe as in the cases of static gain scheduling presented above. There are still a number of cases at very high angles-of-attack that the continuation algorithm failed solve, potentially because higher K_q is required.

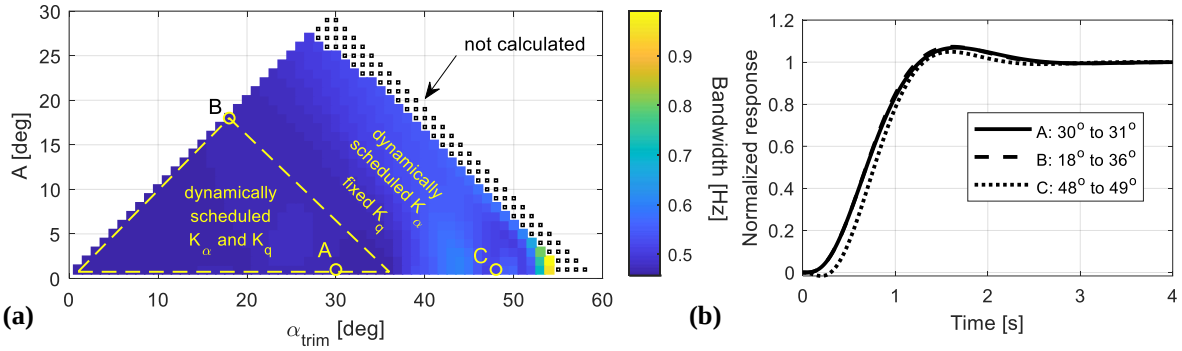

Fig 16 Dynamic gain scheduled controller: (a) closed-loop bandwidth variation and (b) step responses.

The step responses corresponding to points A, B, and C are shown in Figure 16b. Both points A and B lie inside the boundary in which full dynamic gain scheduling is available, with point A highlighting the fact that the control reversal issue previously encountered in Figure 12a has been resolved. In addition, the response in point B – a much more demanding input – is almost identical to what is seen in point A, which shows the advantages of dynamic gain scheduling. The step response at point C, which lies outside the full scheduling region, is also presented. Although the reduction in performance is expected due to the fixed pitch rate feedback gain K_q, the effect is minimal.

VII. Conclusion

This paper highlights the need to develop a nonlinear and closed-loop-based framework for handling qualities assessment. In the first two examples of linearly-designed controllers for a highly nonlinear fighter aircraft model, we have shown that the existence of aerodynamic nonlinearities alone can lead to undesirable responses that cannot be predicted using linear analysis. However, by using nonlinear frequency response analysis to construct the triangular envelope, it is possible to identify regions in which nonlinear behaviors are expected. In particular, the method presented is able to detect the responses that are attracted to a stable isola or can lead to control reversal and high overshoot, none of which is predicted by linear-based analysis. In fact, some of the responses are so nonlinear that it is not possible to represent their dynamics with any linear transfer function, as shown by the closed-loop frequency response in the control-reversal region of the integral controller. Finally, the analysis of dynamic gain scheduling controller ensures that no false-positive results is obtained as well as highlighting the superior performance of the method, which exemplifies a controller designed using nonlinear techniques. The nonlinear frequency response analysis method therefore provides a means of gaining insight into potential degradations in performance and handling qualities when a controller designed using linear techniques is applied to a highly nonlinear system.

Acknowledgements

The first author is partially funded by the University of Bristol's Alumni Grant. The support of QinetiQ in providing the HHIRM flight model is also gratefully acknowledged.

References

1. Richardson, T., Lowenberg, M., Di Bernardo, M., and Charles, G. "Design of a Gain-Scheduled Flight Control System Using Bifurcation Analysis", *Journal of Guidance, Control, and Dynamics*, Vol. 29, No. 2, 2006, pp. 444-453.
doi: 10.2514/1.13902

2. Gill, S. J., Lowenberg, M. H., Neild, S. A., Crespo, L. G., Krauskopf, B., and Puyou, G. "Nonlinear Dynamics of Aircraft Controller Characteristics Outside the Standard Flight Envelope", *Journal of Guidance, Control, and Dynamics*, Vol. 38, No. 12, 2015, pp. 2301-2308.
doi: 10.2514/1.G000966

3. Annonymous. "Military Specification - Flying Qualities of Piloted Airplanes." US Department of Defense, TR-MIL-F-8785C, 1980.

4. Gibson, J. C. "The development of alternative criteria for FBW handling qualities", *AGARD Conference Proceedings No. 508*, AGARD Paper 9, 1991.

5. Carroll, J. V., and Mehra, R. K. "Bifurcation Analysis of Nonlinear Aircraft Dynamics", *Journal of Guidance, Control, and Dynamics*, Vol. 5, No. 5, 1982, pp. 529-536.
doi: 10.2514/3.56198

6. Lowenberg, M. H. "Bifurcation analysis of multiple–attractor flight dynamics", *Philosophical Transactions of the Royal Society of London. Series A: Mathematical, Physical and Engineering Sciences*, Vol. 356, No. 1745, 1998, pp. 2297-2319.
doi: 10.1098/rsta.1998.0275

7. Mehra, R. K., and Prasanth, R. K. "Bifurcation and limit cycle analysis of nonlinear pilot induced oscillations", *23rd Atmospheric Flight Mechanics Conference*, AIAA Paper 144-153, 1998.

8. Gránásy, P., Thomasson, P. G., Sørensen, C. B., and Mosekilde, E. "Non-linear flight dynamics at high angles-of-attack", *The Aeronautical Journal*, Vol. 102, No. 1016, 1998, pp. 337-344.
doi: 10.1017/S0001924000027585

9. Lowenberg, M., and Menon, P. "An Analysable Nonlinear Criterion for Clearance of Flight Control Laws", *AIAA Guidance, Navigation and Control Conference and Exhibit*, Paper 2007.

10. Holmes, P. J., and Rand, D. A. "The bifurcations of Duffing's equation: An application of catastrophe theory", *Journal of Sound and Vibration*, Vol. 44, No. 2, 1976, pp. 237-253.
doi: 10.1016/0022-460x(76)90771-9

11. Cui, F., Chew, C. H., Xu, J., and Cai, Y. "Bifurcation and Chaos in the Duffing Oscillator with a PID Controller", *Nonlinear Dynamics*, Vol. 12, No. 3, 1997, pp. 251-262.
doi: 10.1023/A:1008204332684

12. Nayfeh, A. H., and Sanchez, N. E. "Bifurcations in a forced softening duffing oscillator", *International Journal of Non-Linear Mechanics*, Vol. 24, No. 6, 1989, pp. 483-497.
doi: 10.1016/0020-7462(89)90014-0

13. Kuznetsov, I. A., *Elements of applied bifurcation theory*, 3rd ed., Applied mathematical sciences ; v. 112, Springer, New York, 2004.

14. Strogatz, S. H., *Nonlinear Dynamics and Chaos: with Applications to Physics, Biology, Chemistry, and Engineering*, Addison–Wesley, Reading, MA, 1994.

15. Nayfeh, A. H., and Mook, D. T., *Nonlinear Oscillations*, Nonlinear Oscillations, Wiley, New York, 1979.

16. Gill, S. J., Lowenberg, M. H., Neild, S. A., Krauskopf, B., Puyou, G., and Coetzee, E. "Upset Dynamics of an Airliner Model: A Nonlinear Bifurcation Analysis", *Journal of Aircraft*, Vol. 50, No. 6, 2013, pp. 1832-1842.
doi: 10.2514/1.C032221

17. Goman, M. G., Zagainov, G. I., and Khramtsovsky, A. V. "Application of Bifurcation Methods to Nonlinear Flight Dynamics Problems", *Progress in Aerospace Sciences,* Vol. 33, No. 9-10, 1997, pp. 539-586. doi: 10.1016/S0376-0421(97)00001-8

18. Goman, M., Khramtsovsky, A., and Usoltev, S. "High Incidence Aerodynamics Model for Hypothetical Aircraft," *Technical Rept. 15/5DRA*. Defense Research Agency, Bedford, Bedfordshire, England, UK, 1995.

19. Richardson, T., Davison, P., Lowenberg, M., and Bernardo, M. d. "Control of Nonlinear Aircraft Models Using Dynamic State-Feedback Gain Scheduling", *AIAA Guidance, Navigation, and Control Conference and Exhibit*, Paper 2003.

20. Coetzee, E., Krauskopf, B., and Lowenberg, M. H. "The Dynamical Systems Toolbox: Integrating AUTO into Matlab", *16th US National Congress of Theoretical and Applied Mechanics*, Pennsylvania State University Paper USNCTAM No. USNCTAM2010-827, State College, PA, 2010.

21. Doedel, E. J. "*AUTO-07P, Continuation and Bifurcation Software for Ordinary Differential Equations, Ver. 07P*", http://www.macs.hw.ac.uk/~gabriel/auto07/auto.html [retrieved 11 October 2020].

22. Jones, C. D. C., Lowenberg, M. H., and Richardson, T. S. "Tailored Dynamic Gain-Scheduled Control", *Journal of Guidance, Control, and Dynamics,* Vol. 29, No. 6, 2006, pp. 1271-1281. doi: 10.2514/1.17295

23. Richardson, T. S. "Continuation Methods Applied to Nonlinear Flight Dynamics and Control", PhD thesis, Department of Aerospace Engineering, University of Bristol, Bristol, UK, 2002.